Journal of Power Sources 234 (2013) 197–200

Contents lists available at SciVerse ScienceDirect

Journal of Power Sources

journal homepage: www.elsevier.com/locate/jpowsour

Short communication

$Li_3V_2(PO_4)_3$/C nanofibers composite as a high performance cathode material for lithium-ion battery

Quanqi Chen [a,b,*], Tingting Zhang [b], Xiaochang Qiao [b], Diquan Li [c,**], Jianwen Yang [a]

[a] College of Chemistry and Bioengineering, Guilin University of Technology, Guilin 541004, China
[b] School of Chemistry, Xiangtan University, Xiangtan 411105, China
[c] School of Geosciences and Info-Physics, Central South University, Changsha 410083, China

HIGHLIGHTS

- ► LVP/C nanofibers prepared by electrospinning have surface area of 160.75 $m^2\ g^{-1}$.
- ► The composite exhibits capacity of 190 and 132 mAh g^{-1} at 0.1 C and 20 C, respectively.
- ► Capacity retention of 85.6% is obtained at 20 C after 300 cycles in 3.0–4.8 V.

GRAPHICAL ABSTRACT

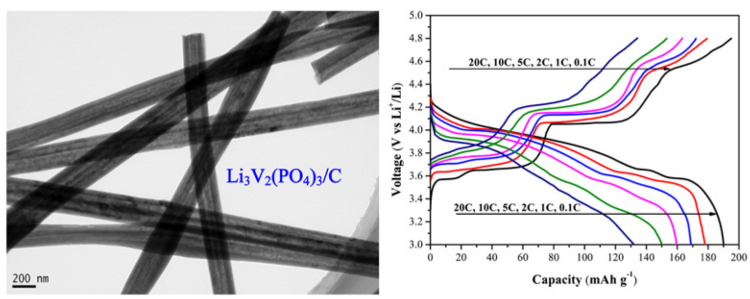

ARTICLE INFO

Article history:
Received 6 December 2012
Received in revised form
27 January 2013
Accepted 29 January 2013
Available online 9 February 2013

Keywords:
Nanofibers
Lithium vanadium phosphate
Electrospinning method
Lithium-ion batteries
Composite

ABSTRACT

A novel $Li_3V_2(PO_4)_3$/C nanofibers composite has been first prepared by a facile and environmentally friendly electrospinning method using NH_4VO_3, CH_3COOLi, poly (4-vinyl) pyridine (PVP) and citric acid aqueous solution as raw materials. The composite is investigated by X-ray diffraction (XRD), scanning electron microscope (SEM), transmission electron microscopy (TEM) and electrochemical tests. The $Li_3V_2(PO_4)_3$/C nanofibers composite exhibits excellent cycle performance and good rate capability in the voltage range of 3.0–4.8 V. The composite displays a high discharge capacity of 190 mAh g^{-1} (close to theoretical capacity of 197 mAh g^{-1}) at 0.1 C (19.7 mA g^{-1}). Even at a high-rate of 20 C, the composite presents the discharge capacity of 132 mAh g^{-1} and good cycle performance. The outstanding electrochemical performance is attributed to the particular morphology and microstructure of $Li_3V_2(PO_4)_3$/C nanofibers composite that dispersive $Li_3V_2(PO_4)_3$ nanofibers and carbon nanofibers aggregate to form nanofibers composite with mesopores and large surface area.

1. Introduction

Lithium-ion batteries are widely considered as the most advanced energy storage systems due to their higher energy conversion efficiencies and energy densities, and longer cycle lives than those of other energy storage systems [1]. The lithium-ion batteries that fulfill a variety of safety, environmental, energy density, power density, cost and cycle life demands are recognized as the potential powers for next generation of plug-in hybrid electric vehicles (PHEVs) and electric vehicles (EVs) [2,3]. As a cathode material for lithium-ion batteries, monoclinic lithium vanadium phosphate, $Li_3V_2(PO_4)_3$ (LVP), has been intensively regarded as one of the most promising candidates with high energy density for high-power lithium-ion batteries because of its high

* Corresponding author. College of Chemistry and Bioengineering, Guilin University of Technology, Guilin 541004, China. Tel./fax: +86 773 5896 446.
** Corresponding author. Tel.: +86 731 8883 6153; fax: +86 731 8883 6783.
E-mail addresses: quanqi.chen@yahoo.com, quanqi.chen@glut.edu.cn (Q. Chen), lidiquan@126.com (D. Li).

0378-7753/$ – see front matter
http://dx.doi.org/10.1016/j.jpowsour.2013.01.164

capacity, good Li^+ mobility, and excellent thermal and cyclic stabilities.

LVP contains stable framework structure and large three-dimensional path for rapid Li^+ diffusion and can theoretically deliver reversible capacity of 197 mAh g^{-1} in the voltage range of 3.0–4.8 V, which corresponds to intercalation/extraction of $3Li^+$ per one molecule [4–6]. However, the poor electronic conductivity [4] (2.0×10^{-8} S cm^{-1}) of LVP degrades its electrochemical performance and significantly limits its practical applications, especially in cases where the rate performance is prerequisite. To overcome this problem, many efforts have been focused on increasing the electronic conductivity of LVP. Previous reports demonstrated that carbon coating on LVP or embedment of LVP into electric carbon network can significantly improve the electronic conductivity, hence to improve the electrochemical performance [5,7–15]. It is well known that both electronic and ionic mobilities in electroactive material are key determinant factors for rate capability and cycle performance in principle. Thus, the combination of improvement of electronic and ionic conductivities is a most effective strategy to improve the electrochemical performance of LVP. The nanosized LVP/C composite can satisfy the requirements of both high electronic and ionic conductivities because the nanosized LVP is kinetically favorable to rapid transport and insertion/extraction of Li^+ in active particles, resulting in high ionic conductivity, and the addition of highly conductive carbon can markedly improve the electronic conductivity. The nanosized composites which consist of electric networks and LVP active materials with different morphologies, such as spherical particles [16], rods [17], belts [18], plates [19] and films [11], have been investigated and proved to have better electrochemical performance.

However, to our knowledge, the fibrous $Li_3V_2(PO_4)_3$/C composite has been not investigated up to date. Whereas, $LiFePO_4$/C nanofibers composite [20–22] showed excellent electrochemical performance even if the electronic conductivity of pristine $LiFePO_4$ is extremely low (about 10^{-9} S cm^{-1}). The special characteristics of nanofibers are responsible for the excellent electrochemical performance of $LiFePO_4$ because nanofibers can provide a much better percolation behavior than particles, and high electronic and ionic conductivities. It is expected that nanofibers will be also beneficial to exceedingly improve the electrochemical performance of LVP. In this work, the novel $Li_3V_2(PO_4)_3$/C nanofibers composite was prepared by a facile and environmentally friendly electrospinning method and it showed excellent electrochemical performance.

2. Experimental

2.1. Synthesis of $Li_3V_2(PO_4)_3$/C nanofibers composite

The typical procedure of preparation of electrospun precursor fibers is as follows: 0.5 g NH_4VO_3 and stoichiometric amount of $NH_4H_2PO_4$ and $CH_3COOLi \cdot 2H_2O$ were added to 5 mL 14 wt% citric acid solution and stirred for 4 h at 60 °C thermostatic bath to obtain homogeneous solution. Then, the resulted solution was dropped slowly into the mixture solution of 1.0 g poly (4-vinyl) pyridine (PVP) (Alfa Aesar, $M_w = 1{,}300{,}000$) and 4.0 g H_2O, and stirred for 4 h to get a homogeneous viscous electrospinning solution. The electrospinning solution was loaded into a plastic syringe equipped with a steel needle of 0.6 mm in internal diameter and the ejection rate of electrospinning solution from the syringe was 0.25 mL h^{-1}. The applied voltage for electrospinning was 32 kV. The flat aluminum foil was placed 20 cm below the needle tip to collect the composite fibers. The precursor composite fibers were collected, dried at 90 °C for 12 h under vacuum, calcined at 800 °C for 4 h in Ar atmosphere at a ramp rate of 2 °C min^{-1}, cooled to room temperature to yield $Li_3V_2(PO_4)_3$/C nanofibers composite (NF-LVP/C).

2.2. Physical characterizations

The crystal structure of the resulted composite was determined by an X-ray diffractometer (XRD; Rigaku 2500). The carbon content of the composite was determined by a carbon–sulfur analyzer (Mlti EA2000). The morphology and microstructure of the products were observed by a scanning electron microscope (SEM; JSM-5600LV) and a transmission electron microscopy (TEM; JEOL JEM2010). N_2 adsorption/desorption measurement was performed by a Nova Station B (Quantachrome).

2.3. Electrochemical measurements

Electrochemical experiments were performed with 2032 coin cells using Li foil as counter and reference electrodes. The working electrode was prepared by mixing NF-LVP/C, acetylene black (Timcal), and polyvinylidiene fluoride (PVDF, Atofina) at a weight ratio of 80:10:10 in *N*-methylpyrrolidone (NMP). The resultant slurry was then uniformly pasted on aluminum foil current collector and dried at 120 °C for 24 h in a vacuum oven. The mass loading of active material was about 2.5–3.0 mg cm^{-2} and the thickness of electrode materials on the current collector was about 30–40 μm. The Polypropylene film (Celgard 2400) was used as a separator. The electrolyte was 1 M $LiPF_6$ dissolved in the mixture of ethyl carbonate and dimethyl carbonate (1:1 by volume) (Merck). The coin cells were assembled in an argon-filled glove box and galvanostatically cycled at different current densities (1 C = 197 mA g^{-1}) in the voltage range of 3.0–4.8 V at 25 °C using a NEWARE battery testing system. The cells were charged to 4.8 V then discharged to 3.0 V, and the discharge rate was the same as the charge rate during every cycle. The specific capacity and current density were calculated based on the mass of active material.

3. Results and discussion

Fig. 1 shows the morphologies of precursor and LVP/C composite. The dispersive precursor fibers are clearly observed in Fig. 1a, the fibrous structure is maintained even after the precursor was calcined at 800 °C for 4 h to form LVP/C (Fig. 1b). However, the diameters of fibers decrease from 170 to 410 nm for precursor fibers to 90–220 nm for LVP/C fibers. This change is attributed to pyrolysis of organic compounds and the suppression of the growth and aggregation of LVP crystals by in-situ carbon. The TEM image (Fig. 1c) reveals the observed diameters of dispersive NF-LVP/C are in the range of 151–220 nm, in accordance with the SEM observation (Fig. 1b). HRTEM in the inset of Fig. 1c presents clear lattice fringe with d-space of 0.384 nm, corresponding to (102) plane of monoclinic LVP. Although carbon content is about 4.3 wt% in NF-LVP/C, no distinct coating carbon or carbon fibers can be observed in Fig. 1c, even in high magnification and partially enlarged TEM images (Fig. 1d), which may suggest that both carbon and LVP fibers are evenly dispersive in NF-LVP/C. Unlike the carbon coated LVP, this special microstructure of NF-LVP/C may be more favorable to improve electronic conductivity of the composite.

A porous morphology of NF-LVP/C is obviously observed in Fig. 1d, and the porous structure is investigated by N_2 adsorption/desorption isotherm. The typical type-IV isotherm shown in Fig. 2a further indicates a mesoporous structure of the NF-LVP/C. The Barrett–Joyner–Halenda (BJH) pore-size distribution presented in inset of Fig. 2a suggests that composite contains broadly distributed pores with sizes below 100 nm and a large number of pores are mesopores with diameters of 2–20 nm. The total pore volume of the composite is as high as 0.328 cm^3 g^{-1}. The high pore volume and ample mesopores allow electrolyte rapidly flood in and facilitate transport and electrochemical reaction of Li^+ during charge

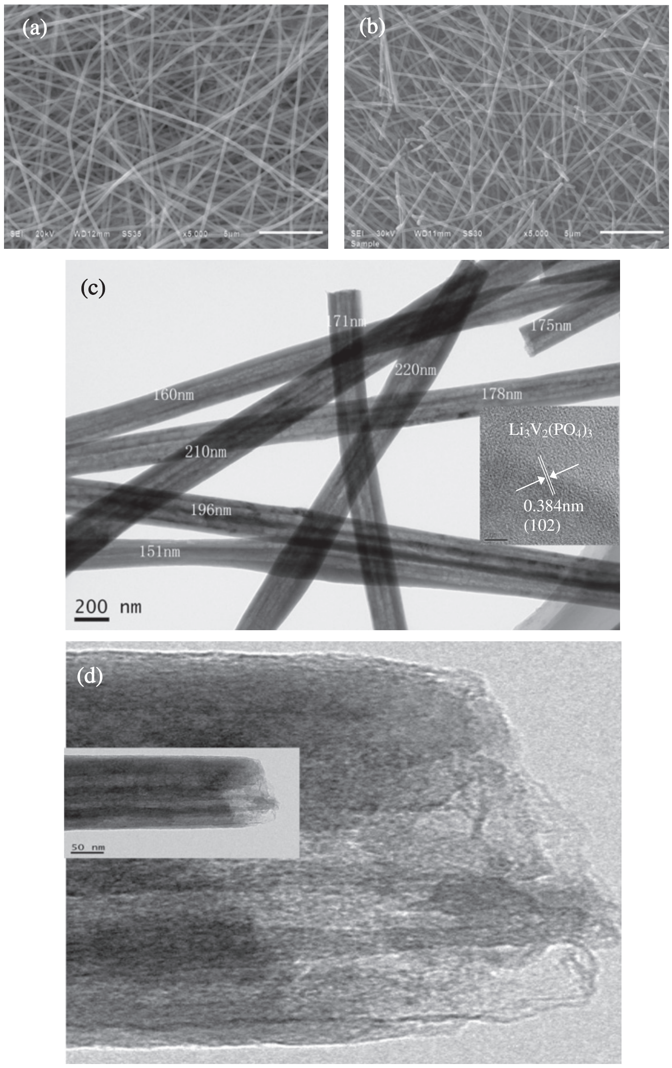

Fig. 1. SEM images of (a) dried precursor and (b) $Li_3V_2(PO_4)_3$/C composite, TEM images of $Li_3V_2(PO_4)_3$/C composite at (c) low and (d) high magnifications. The lattice fringe of $Li_3V_2(PO_4)_3$ is shown in inset of (c).

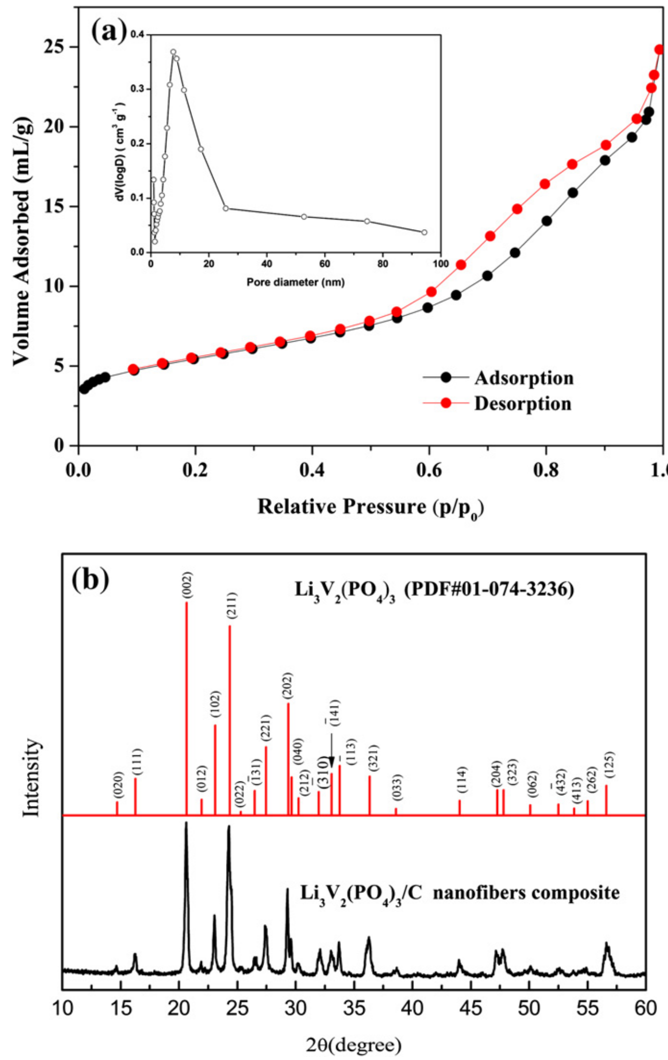

Fig. 2. (a) N_2 adsorption/desorption isotherm, the pore-size distribution curve corresponding BJH (inset), (b) XRD pattern of $Li_3V_2(PO_4)_3$/C nanofibers composite.

and discharge processes. Additionally, the amazing Brunauer–Emmett–Teller (BET) specific surface area of 160.75 $m^2\ g^{-1}$ is obtained. It is expected that this nanoporous structure and large surface area are in favor of improvement of electronic conductivity, electrolyte penetration and diffusion rate of Li^+, resulting in the improved electrochemical performance.

XRD pattern of NF-LVP/C is present in Fig. 2b and all diffraction peaks of this composite can be indexed by well-defined monoclinic phase, in agreement with monoclinic $Li_3V_2(PO_4)_3$ (PDF 01-074-3236). The cell parameters for the composite are as follows: $a = 0.8610$ nm, $b = 1.2052$ nm, $c = 0.8608$ nm and $\beta = 90.5°$. The average crystal size calculated by Debye–Scherrer equation is about 29 nm and this smaller crystal favors formation of smaller NF-LVP/C.

Fig. 3a depicts the charge/discharge profiles of NF-LVP/C electrode at different current rates (1 C = 197 mA g^{-1}) in the voltage range of 3.0–4.8 V at 25 °C. When the cell is charged at 0.1 C, four clear charge plateaus occur at about 3.59, 3.67, 4.08 and 4.57 V, respectively, which corresponds to the extraction of three lithium-ion from LVP over four two-phase transformation [6], while the corresponding discharge curve exhibits two distinct plateaus at about 3.58 and 3.65 V and a sloping plateau about 4.0 V due to the solid solution behavior of insertion first lithium-ion into $V_2(PO_4)_3$ [6]. It is noted that the charge and discharge capacities of NF-LVP/C are 195 and 190 mAh g^{-1} at 0.1 C, close to 99% and 96% of theoretical capacity of 197 mAh g^{-1} for LVP, respectively and the coulombic efficiency is as high as 97.3%, indicating exceptionally high conversion of this active material. The capacity of NF-LVP/C at 0.1 C is higher than those of previous reported particulate LVP/C composites [9,15,23–27], but somewhat lower than 193.7 mAh g^{-1} of plate-like LVP/C composite [19]. Although the discharge capacities decrease with the increasing current rates due to the higher polarization at higher current densities, NF-LVP/C still exhibits high discharge capacities of 178, 169 and 160 mAh g^{-1} at relatively smaller current rates of 1, 2 and 5 C, respectively, higher than those of LVP/graphene (152 mAh g^{-1} at 2 C) [28], plate-like LVP/C (133.1 mAh g^{-1} at 3 C) [19] and LVP/C/graphene (164 mAh g^{-1} at 2 C, 145 mAh g^{-1} at 5 C) [28]. Even at much higher current rates of 10 and 20 C, competitive capacities of 150 and 132 mAh g^{-1} for NF-LVP/C can be achieved, respectively and the values approach to those of the reported best LVP cathode materials, porous LVP/C [14,15] and LVP/C/graphene [28], suggesting that NF-LVP/C possesses high capacity and rate capability.

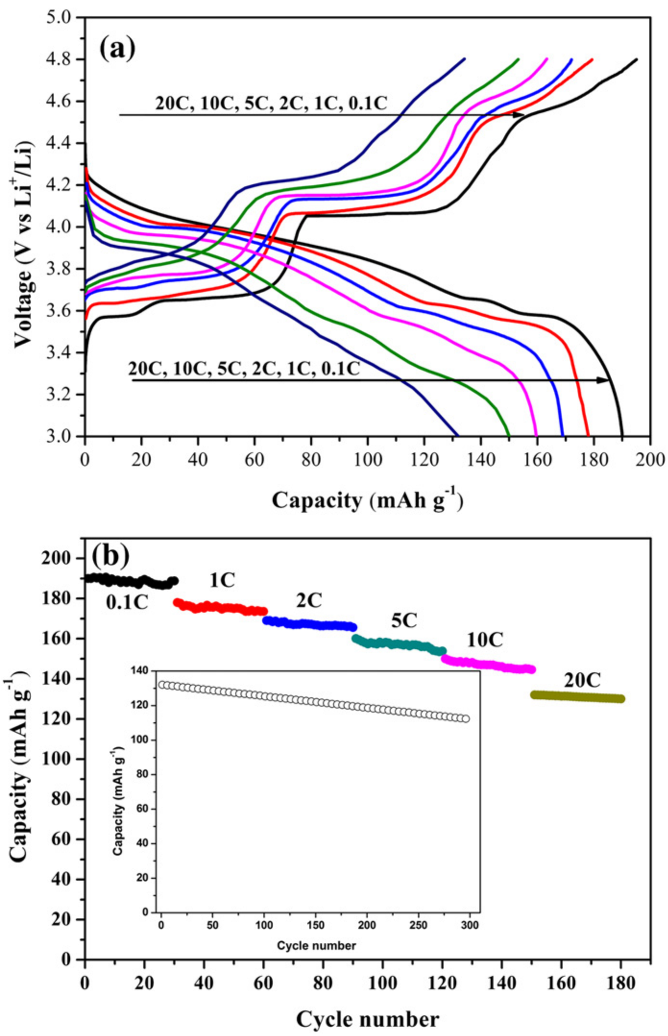

Fig. 3. (a) Charge/discharge profiles of $Li_3V_2(PO_4)_3$/C nanofibers composite at different current rates (1 C = 197 mA g^{-1}), (b) cycle performance of $Li_3V_2(PO_4)_3$/C nanofibers composite at different current rates with the inset showing long term cycle performance of a fresh cell at 20 C.

The cycle performance of NF-LVP/C at different current rates from 0.1 to 20 C illustrated in Fig. 3b reveals that this composite exhibits excellent cycle performance in the voltage range of 3.0–4.8 V. At lower current rates (≤1 C), the capacity retentions are close to 100% after 30 cycles. Even at high-rate of 20 C, the capacity retention is as high as 98.5% and the NF-LVP/C still remains a discharge capacity of 130 mAh g^{-1} after 30 cycles. The inset in Fig. 3b shows the cycle performance of fresh NF-LVP/C electrode at 20 C and a high discharge capacity of 113 mAh g^{-1} is still obtained after 300 cycles, corresponding to the capacity retention of 85.6% which is somewhat higher than that of porous $Li_3V_2(PO_4)_3$/C [14,15].

The outstanding electrochemical performance of NF-LVP/C is attributed to the particular morphology and structure of NF-LVP/C that dispersive LVP nanofibers and carbon nanofibers aggregate to form nanofibers composite with mesopores and large surface area, and the reasons for that are as follows: (1) LVP nanofibers provide short diffusion pathway for Li^+ insertion/extraction; (2) dispersive carbon nanofibers offer high electronic conductivity and facilitate the charge transfer within the electrode and to the current collector, moreover, elastic carbon nanofibers can buffer the volume expansion (8.4%) [4] during cycling to avoid active material depart from the collector; (3) the mesopores and large surface area favor fast transport of electrolyte to active material and increase active sites for Li^+. At the same time, large surface area facilitates much smaller local current density than the operating current density and rapid charge transfer, leading to smaller polarization.

4. Conclusions

A novel $Li_3V_2(PO_4)_3$/C nanofibers composite is prepared by a facile and environmentally friendly electrospinning method. This nanofibers composite exhibits good high-rate performance and cyclic stability in the voltage range of 3.0–4.8 V. The particular microstructure of nanofibers composite is responsible for the outstanding electrochemical performance of $Li_3V_2(PO_4)_3$/C nanofibers composite, which suggests that electrospinning may be an effective method to produce other nanofibers electrode materials with excellent electrochemical performance.

Acknowledgments

This work was financially supported by Hunan provincial Natural Science Foundation of China (No. 12JJ3017), the Open-End Fund for the Valuable and Precision Instruments of Central South University (No. CSUZC2012016), and NSFC (No. 51164006).

References

[1] J.-M. Tarascon, M. Armand, Nature 414 (2001) 359–367.
[2] P.G. Bruce, B. Scrosati, J.-M. Tarascon, Angew. Chem. Int. Ed. 47 (2008) 2930–2946.
[3] B. Kang, G. Ceder, Nature 458 (2009) 190–193.
[4] S.C. Yin, H. Grondey, P. Strobel, M. Anne, L.F. Nazar, J. Am. Chem. Soc. 125 (2003) 10402–10411.
[5] H. Huang, S.-C. Yin, T. Kerr, N. Taylor, L.F. Nazar, Adv. Mater. 14 (2002) 1525–1528.
[6] M.Y. Saidi, J. Barker, H. Huang, J.L. Swoyer, G. Adamson, J. Power Sources 119–121 (2003) 266–272.
[7] M.Y. Saidi, J. Barker, H. Huang, J.L. Swoyer, G. Adamson, Electrochem. Solid State Lett. 5 (2002) A149–A151.
[8] P. Fu, Y. Zhao, X. An, Y. Dong, X. Hou, Electrochim. Acta 52 (2007) 5281–5285.
[9] Q. Chen, J. Wang, Z. Tang, W. He, H. Shao, J. Zhang, Electrochim. Acta 52 (2007) 5251–5257.
[10] J.-C. Zheng, X.-H. Li, Z.-X. Wang, H.-J. Guo, Q.-Y. Hu, W.-J. Peng, J. Power Sources 189 (2009) 476–479.
[11] L. Wang, L.-C. Zhang, I. Lieberwirth, H.-W. Xu, C.-H. Chen, Electrochem. Commun. 12 (2010) 52–55.
[12] X. Du, W. He, X. Zhang, Y. Yue, H. Liu, X. Zhang, D. Min, X. Ge, Y. Du, J. Mater. Chem. 22 (2012) 5960–5969.
[13] C. Wang, H. Liu, W. Yang, J. Mater. Chem. 22 (2012) 5281–5285.
[14] L. Zhang, H. Xiang, Z. Li, H. Wang, J. Power Sources 203 (2012) 121–125.
[15] X. Rui, D. Sim, K. Wong, J. Zhu, W. Liu, C. Xu, H. Tan, N. Xiao, H.H. Hng, T.M. Lim, Q. Yan, J. Power Sources 214 (2012) 171–177.
[16] X.Y. Wang, S.Y. Yin, K.L. Zhang, Y.X. Zhang, J. Alloys Compd. 486 (2009) L5–L9.
[17] H.W. Liu, C.X. Cheng, X.T. Huang, J.L. Li, Electrochim. Acta 55 (2010) 8461–8465.
[18] A. Pan, D. Choi, J.-G. Zhang, S. Liang, G. Cao, Z. Nie, B.W. Arey, J. Liu, J. Power Sources 196 (2011) 3646–3649.
[19] Y.Q. Qiao, X.L. Wang, Y.J. Mai, J.Y. Xiang, D. Zhang, C.D. Gu, J.P. Tu, J. Power Sources 196 (2011) 8706–8709.
[20] E. Hosono, Y. Wang, N. Kida, M. Enomoto, N. Kojima, M. Okubo, H. Matsuda, Y. Saito, T. Kudo, I. Honma, H. Zhou, ACS Appl. Mater. Int. 2 (2010) 212–218.
[21] C. Zhu, Y. Yu, L. Gu, K. Weichert, J. Maier, Angew. Chem. Int. Ed. 50 (2011) 6278–6282.
[22] Q. Chen, X. Qiao, C. Peng, T. Zhang, Y. Wang, X. Wang, Electrochim. Acta 78 (2012) 40–48.
[23] L. Zhang, X.L. Wang, J.Y. Xiang, Y. Zhou, S.J. Shi, J.P. Tu, J. Power Sources 195 (2010) 5057–5061.
[24] Y.Q. Qiao, J.P. Tu, J.Y. Xiang, X.L. Wang, Y.J. Mai, D. Zhang, W.L. Liu, Electrochim. Acta 56 (2011) 4139–4145.
[25] Y.Q. Qiao, X.L. Wang, J.Y. Xiang, D. Zhang, W.L. Liu, J.P. Tu, Electrochim. Acta 56 (2011) 2269–2275.
[26] C.X. Chang, J.F. Xiang, X.X. Shi, X.Y. Han, L.J. Yuan, J.T. Sun, Electrochim. Acta 54 (2008) 623–627.
[27] L.A. Wang, X.Q. Jiang, X. Li, X.Q. Pi, Y. Ren, F. Wu, Electrochim. Acta 55 (2010) 5057–5062.
[28] H. Liu, P. Gao, J. Fang, G. Yang, Chem. Commun. 47 (2011) 9110–9112.